

Finite Element Modeling of a Stone Layer Under a Strip Footing to Estimate Soil Behavior and Determine Optimal Stone Layer Width and Depth

Babak KARIMI ^{1,*}

¹ Department of Civil Engineering, Erzurum Technical University, Erzurum, 25050, Türkiye, **ORCID:** 0000-0001-7897-9085

Article Info

Research paper

Received : May 27, 2022

Accepted : August 3, 2022

Keywords

FEM
Finite Element Method
Plaxis
Soil Improvement

Abstract

Various methods can be applied to improve soil behavior in order to increase the bearing capacity or reduce the settlement of footings. These methods can be categorized as stabilization or improvement of soil by use of different geosynthetics; injection methods; grouting or replacing weak soil with stronger materials. One of the most common methods and materials that can be used for improving soils, is placing a stone layer under the footing. In this study, a stone layer under a strip footing is simulated with the finite element method (FEM) to estimate the soil behavior in different conditions. A strip footing with a width of 1m and length of 8m with a 100 kN/m² uniform load was modelled. Different widths of stone layer from 1B to 3B (B was the strip footing width) with different depths of 0.5B, 1B, 1.5B, and 2B were modelled in Plaxis 3D and results were obtained from the simulation. By reviewing the results, it was found that the optimum dimensions of the stone layer to place under the presented strip footing was 2B width and 1B depth. This result can be applied to real projects with similar conditions.

1. Introduction

Having more settlement and less bearing capacity of soil is the most common problem in foundation applications. There are different methods and strategies in use to improve soil bearing capacity or settlement of footing in weak soils. For example, improving soils by injection or grouting, piles, stone columns, compaction or using stone layers under footing can be applied as some alternative procedures for improving soil properties to increase bearing capacity or reduce the settlement of soil [1].

Plastic piles, stone blockage, and stone columns are some of the most common methods used in recent years to improve the soil structure. Several theoretical and experimental studies were done to simulate and test various methods to evaluate the soil behavior under different conditions of dimension and loading [2-4].

Improving the soil and creating a stronger layer under the footing is one of the methods that can be used to

improve the geotechnical properties of soil under footings. This stronger layer will transfer the loads to the under layers and will positively affect the shear failure surfaces and bearing capacity of the soil. Additionally, it can also reduce the vertical and lateral displacements of soil. Different methods and materials can be used for improving the soil [5-8]. Fiber reinforced soils, geosynthetic-reinforced soils, and compaction in a variety of ways [9-11] can be given as examples. There are different numerical methods to understand the soil's behavior at different conditions. The Finite element method (FEM) is one of the most commonly used methods for simulating geotechnical problems. Different conditions and materials can be modelled with different software[12-14].

The type of soil and foundation must be taken into consideration when selecting the improvement method. Experiments can be carried out on both granular and fine cohesive soils. In a study, direct shear tests were applied to study the mechanisms of fiber reinforcement [15]. Different materials were used for reinforcing the soil, for example, granular soils were reinforced with fiber to investigate the effects of reinforcement [16]. Results of this work showed that the reinforcement of granular soil with

* Corresponding Author: babak.karimi@erzurum.edu.tr



fiber was more effective in fine graded than in medium-grained sands. At the same time, the effect of reinforcement was more considerable with sub-rounded particles in comparison to sub-angular particles [16].

One of the methods that can be applied to weak soil with engineering problems is removing the weak soil and replacing it with stronger soil or materials. In this case, the weak layer of soil under the footing can be replaced with a stone layer at a different depth and width. In this study, a strip footing lying on weak soil was modeled with the Plaxis 3D software, and weak soil under the footing was replaced with a strong stone layer to obtain the optimum depth and width of the new replaced stone mass.

2. Materials and Methods

In this study, three kinds of soil materials were used for modelling and simulation. A soft, weak, sandy soil, a stone mat used beneath the footing as a stone layer, and concrete for the footing. The Mohr-Coulomb model was used to simulate the sand and stone in the drained condition that has been used in similar previous studies [17-19]. As the stone blockage is not massive rock and the behaviour of this improved layer is not similar to rock with cracks inside rock mass or stone blocks, Mohr-Coulomb was chosen for material type in the simulation. A strip footing with a dimension of 1*8 m was modeled in this study. The footing was put on a drained, weak sandy soil. A 100 kN/m² uniform load was applied to the model footing, and the maximum vertical settlement and shear failure mechanism of the soil under the footing were investigated. At the next step, weak soil under footing was replaced with a stone layer with different depths and width, and the behavior, shear failure mechanism, and settlements were compared with normal conditions. Plaxis 3D finite

element software was used for modeling the footing, soil, and stone.

The finite element method was developed for simulating various engineering analyses for modeling and analyzing complex systems in the area of civil and mechanical engineering. Seven material parameters are used to define the materials associated with this model, namely unsaturated unit weight (γ_{unsat}), saturated unit weight (γ_{sat}), Young's modulus (E), Poisson's ratio (ν), effective friction angle (ϕ'), effective cohesion (c') and dilation angle (ψ). A stone layer is defined as a uniformly drained soil material. The footing used for the simulation was a rigid concrete footing with a thickness of 80 cm. The soil used for the modeling was a weak soil that caused big settlements under loading of footing. The properties of footing, soil, and stone are presented in Table 1.

A strip footing was simulated with FEM. The width (B) and length (L) of the footing are 1 and 8 m, respectively. The first simulation was done without any stone layer under the footing, and vertical deformation of soil and shear failure surfaces were obtained. Then a strong stone layer with a width of strip footing (B) and a depth of 0.5B was placed under the footing and simulated again. After that, by increasing the depth of the stone layer, a strip footing was modeled with a stone layer of 1B, 1.5B, and 2B. At the next step, the width of the stone layer was increased on two sides. This increment was 0.5B and 1B on each side. In other words, four different depths of 0.5B, 1B, 1.5B, and 2B with three different widths of B, 2B, and 3B of stone layer were simulated under a strip footing with constant width and uniform loading. And finally, maximum deformation and soil behavior at each condition were studied. The schematic shape of the foundation and stone blockage under footing is shown in figure 1.

Table 1. Properties of Elements Used for FEM Modelling

Parameter	Unit	Value		
		Soil	Stone	Strip Footing
Model		Mohr-Coulomb	Mohr-Coulomb	-
Unsaturated Unit Weight	(kN/m ³)	17	19	-
Saturated Unit Weight	(kN/m ³)	18.5	21	-
Young's Modulus	(kN/m ²)	8500	45000	-
Poisson's Ratio		0.15	0.1	-
Cohesion	(kN/m ²)	1	1	-
Friction Angle	°	30	40	-
Dilation Angle	°	30	10	-
Material type		-	-	Elastic and Isotropic
d	m	-	-	0.8
Unit Weight	(kN/m ³)	-	-	20
Young's Modulus	(kN/m ²)	-	-	32x10 ⁶

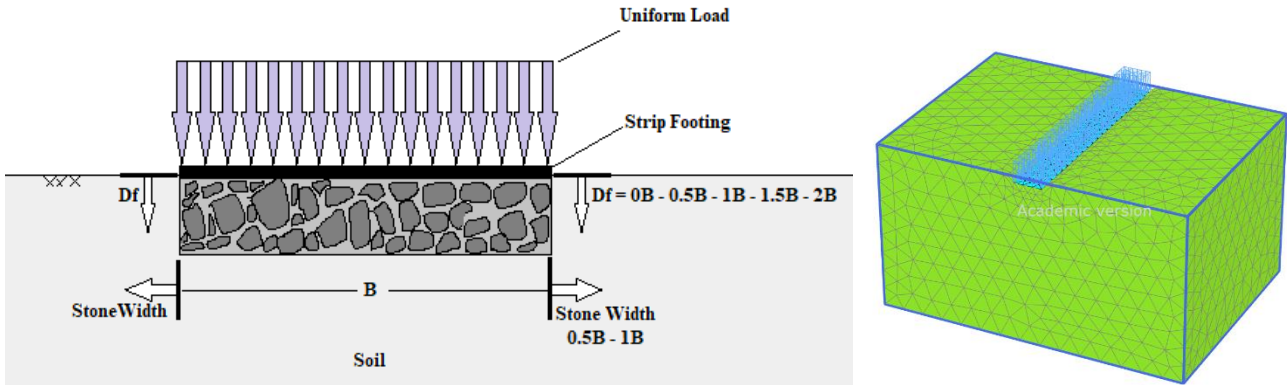


Figure 1. Schematic Shape of Foundation and Stone Blockage Modelling

In the material properties definition, the value of R_{inter} at the interface is 0.95 for sand and 1 for stone. As the simulations were done at drained conditions, the head of water for soil layers was at the bottom of the total soil layers. Therefore, as there was no water level in the simulation, the effect of an increase or decrease in water level was not taken into consideration. The mesh generated for simulation is a medium-sized mesh that is finer under footing. Plaxis 3D applied boundary conditions automatically and as there were no special conditions, the default boundary conditions did not change. In Plaxis modeling, the width of the stone layer was increased by $0.5B$ from each side of the footing to obtain a $2B$ width, and at the next step, $0.5B$ was added to the width once again to estimate a $3B$ stone layer width. The depth of the stone layer increased by $0.5B$ at each step, and four different depths of $0.5B$, $1B$, $1.5B$ and $2B$ of stone depth were simulated. At the simulation's staged construction step, the calculation type was "K0 procedure." Three phases were performed for the analysis, such as defining the soil and stone layer volumes, placing the plate as a foundation, and finally applying the 100 kN/m^2 uniform load. For soil properties, the value of Young's Modulus was entered as 8500 kN/m^2 , cohesion of 1 kN/m^2 and friction angle of 30° , which defines a weak, loose sandy soil.

3. Results and Discussion

The strip footing under a load of 100 kN/m^2 was modeled and simulated, and results containing maximum displacements and shear failure surfaces were obtained from the models. Figure 2 shows the total displacement of soil under the load of a footing. As seen in this figure, punching shear failure surfaces happened in normal soil without any stone layer. That is because of the loose structure of soil.

In continuation, stone layers were placed under strip footing at different depths and widths. Figure 3 shows the

displacement of soil and stone layer with $1B$ width at different depths. Because of the plane strain condition in simulation and to better view the shear failure mechanism of soil, all figures were shown perpendicular to the third dimension in 2D format.

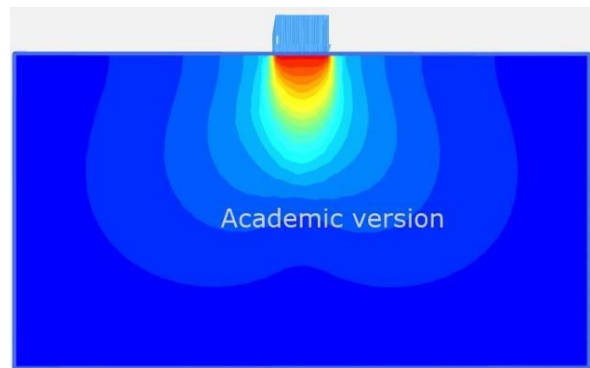


Figure 2. Total Displacement of Soil Mass without any Blockage

As seen in figure 3, by increasing the depth of the stone layer, the total affected depth of soil did not change significantly, but the punching areas were moved down and, due of the stronger materials used in the stone layer, the shear failure surfaces on two sides of this strong layer were more considerable than those inside it.

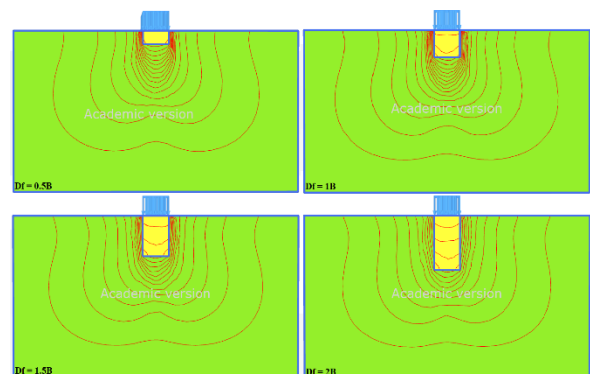


Figure 3. Shear Failure Surfaces of Soil and Stone Layers with B Width and Different Depths

But generally, the failure surface was punching at different depths. Continuing by increasing the width of the stone layer to 2B (1B under footing and 0.5B from each side of footing), different conditions were simulated and the results are shown in figure 4.

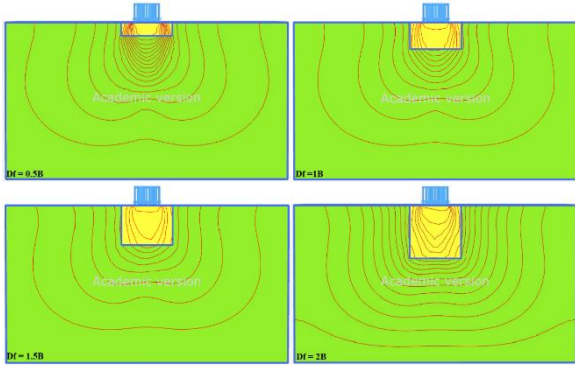


Figure 4. Shear Failure Surfaces of Soil and Stone Layers with 2B Width and Different Depths

In the stone layer modelling with 2B width and 0.5B depth, the failure surface was punching too, and even main stresses were seen in the stone mass. But by increasing the depth of stone, local shear failure surfaces started to form, and the load was distributed over a wider area under the footing. But the most critical area was still under the footing, and placing the stronger stony layer under the footing helped the total soil mass carry the applied load.

Finally, the width of the stone layer under footing increased to 3B (1B under footing and 1B from each side of footing) and 4 different conditions with the same loading and strip properties were simulated in Plaxis 3D and the results are shown in figure 5. In the condition of 0.5B depth, like all other conditions of stone mass width, the failure surfaces were punching. But as the depth of stone increased, the type of failure surface moved toward the local failure surface. In a stone mass with 3B width and 2B depth, the main load is carried by a stone layer that can lead to the increasing of the bearing capacity and fewer settlements. Settlements of footing in different conditions of stone layer width and depth were shown in figures 6 and 7. Figure 6 shows the settlement via stone layer depth and Figure 7 shows the settlement changed by stone layer widths.

The amount of settlement before placing any stone layer under the footing was 49 mm. As it is seen in previous studies, this settlement can be in an acceptable range, but as the main object of this paper is studying the effect of stone blockage, the effect of soil improvement was investigated by placing stone under the footing. As seen in figures 6 and 7, the settlement is reduced by increasing the width and depth of the stone layer. A rigid strip footing was simulated in this paper, so settlements in the corner and middle of the footing were equal.

As it can be deduced from the results, the settlement decreased from 49mm to 40mm by using a stone layer with a 1B width and 0.5B depth. The amount of settlement was 34, 29 and 25 mm while the depth of the stone layer increased to 1B, 1.5, and 2B respectively.

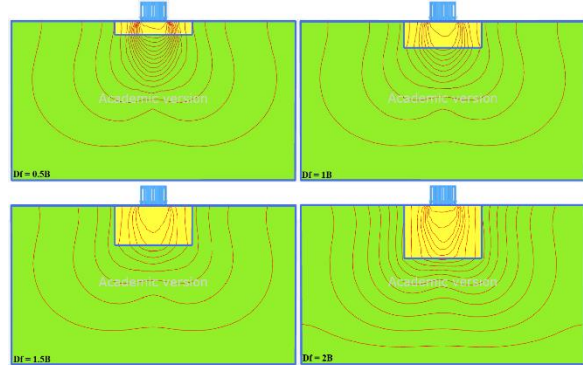


Figure 5. Shear Failure Surfaces of Soil and Stone Layers with 3B Width and Different Depths

By increasing the width of this stronger layer, settlement reached 36mm at 0.5B depth. It decreased to 25, 21, and 17mm while the stone blockage depth was 1B, 1.5B, and 2B respectively.

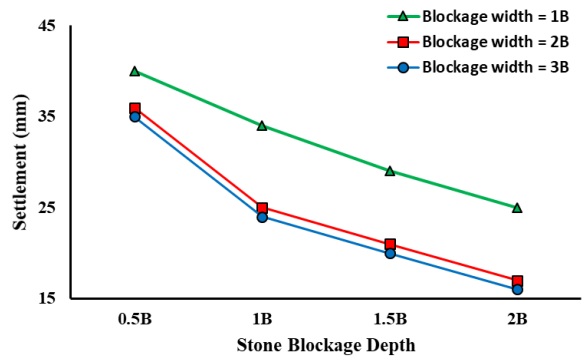


Figure 6. Settlement of footing changed with Stone Blockage Depth

Increasing the blockage width to 3B led to a decrease in settlement of the footing, but the differences were not so considerable. The amount of settlement in 3B blockage width was 35, 24, 20, and 16mm in depths of 0.5B, 1B, 1.5B, and 2B respectively.

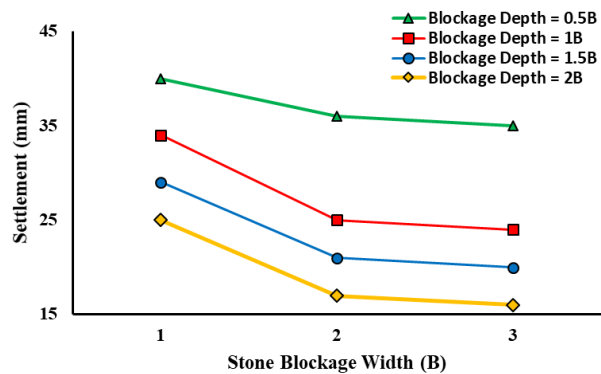


Figure 7. Settlement of footing changed with Stone Blockage Width

Figure 7 shows the change of footing settlement by stone layer width at different stone layer depths. As seen in this figure, the difference between 0.5B and 1B depth and 1B and 2B blockage width was more considerable than in other conditions, and after the width of 2B, the amount of settlement did not change significantly. The settlements of footing in different conditions are presented in Table 2.

Table 2. Settlement of Footing at Different Conditions

Depth	Settlement (mm)			
	Stone Blockage Width			
	0B	1B	2B	3B
0.5B	49	40	36	35
1B	49	34	25	24
1.5B	49	29	21	20
2B	49	25	17	16

4. Conclusions

By reviewing the results of shear failure surfaces and settlements, it was found that placing a stone layer under strip footing will reduce the settlement of the foundation and change the shear failure surface of soil. Generally, increasing the width and depth of the stone layer in all conditions reduced the settlement, but there were not so many differences in the settlement of footing in 2B and 3B widths. Additionally, settlement between 2B and 3B width of the stone layer was not so considerable. Therefore the optimum width and depth that can be selected for the simulated stone layer can be decided as 2B width (1B + 0.5B from each side of the footing) and 1B depth. In applications with similar conditions these dimensions can be selected as the optimum dimensions for the stone layer under strip footings.

This manuscript helps better understand the behaviour of improved soil layers under strip footings. The results can be used for choosing the optimum depth and width of stone blockage under footings under the conditions presented in this paper.

Declaration of Ethical Standards

The author of this article declares that the materials and methods used in this study do not require ethical committee permission or legal-special permission.

Conflict of Interest

The author declares that they have no known competing financial interests or personal relationships that could have appeared to influence the work reported in this paper.

Acknowledgements

The author thanks so much to Erzurum Technical University for providing Plaxis 3D software for using and simulating the model.

References

- [1] Bergado D. T., Anderson L. R., Miura N., 1994. Balasubramaniam AS., ASCE press, **4**, 427.
- [2] Lo S. R., Zhang r., Mak j., 2010. Geosyntheticencased stone columns in soft clay: A numerical study. *Geotextiles Geomembranes*, **28**, pp. 292-302.
- [3] Al-Kaisi, A. A. R., Ali H. H., 2013. Mathematical estimation for the bearing capacity of sand column inserted in soft clay soil. *Eng. Technol. J.*, **31**, pp. 816-827.
- [4] Al-Saoudi N. K. S., Al-Kaissi M. M., Rajab N. A. A., 2014. Treatment of soft soil by sand columns. *Eng. Technol. J.*, **32**, pp. 2106-2118.
- [5] Sánchez-Garrido A. J., Navarro I. J., Yepes V., 2022. Evaluating the sustainability of soil improvement techniques in foundation substructures. *Journal of Cleaner Production*, **1**(351), pp.131463.
- [6] Bagriacik B., 2021. Utilization of alkali-activated construction demolition waste for sandy soil improvement with large-scale laboratory experiments. *Construction and Building Materials*, **4**(302), pp.124-173.
- [7] Naghizadeh A., Ekolu S. O., 2022. Activator - related effects of sodium hydroxide storage solution in standard testing of fly ash geopolymer mortars for alkali – silica reaction. *Materials and Structures*, **55**(22), pp. 1-16. <https://doi.org/10.1617/s11527-021-01875-8>
- [8] Naghizadeh A., Ekolu S. O., 2021. Effects of compositional and physico – chemical mix design parameters on properties of fly ash geopolymer mortars. *Journal of Silicon*, **13**(12), pp. 4669-4680. <https://doi.org/10.1007/s12633-020-00799-2>
- [9] Zornberg J. G., 2002. Peak versus residual shear strength in geosynthetic-reinforced soil design. *Geosynthetics International*, **9**(4), pp. 301-318. <https://doi.org/10.1680/gein.9.0220>
- [10] Murray J. J., Frost J. D., Wang Y., 2000. Behavior of a sandy silt reinforced with discontinuous recycled fiber inclusions, *Recycled and Secondary Materials. Soil Remediation, and in Situ Testing*, **1714**, pp. 9-17, *Transportation Research Record*.

- [11] Consoli N. C., Montardo J. P., Prietto P. D. M., Pasa G. S., 2002. Engineering behavior of a sand reinforced with plastic waste. *J. of Geotech. and Geoenviron. Engrg., ASCE*, **128**(6), pp. 462-472.
- [12] Yu Y., Damians I. P., Bathurst R. J., 2015. Influence of choice of FLAC and PLAXIS interface models on reinforced soil–structure interactions. *Computers and Geotechnics*, **1**(65), pp.164-174.
- [13] Wulandari P. S., Tjandra D., 2015. Analysis of geotextile reinforced road embankment using PLAXIS 2D. *Procedia Engineering*, **1**(125), pp. 358-362.
- [14] Srivastava S., Sinha A., Kumar R., 2022. Simulating the assembly size on seismic response of building clusters using PLAXIS. *Materials Today: Proceedings*.
- [15] Gray D. H., Ohashi H., 1983. Mechanics of fiber-reinforcement in sand. *J of Geotech Engrg., ASCE*, **109**(3), pp.335-353.
- [16] Al-Refeai T. O., 1991. Behavior of antigranulocytes soils reinforced with discrete randomly oriented inclusions. *Geotextiles and Geomembranes*, **10**(4), pp. 319-333.
- [17] Yoo C., 2015. Settlement Behaviour of Embankment on Geosynthetic-Encased Stone Column Installed Soft Ground - A Numerical Investigation. *Geotextiles and Geomembranes*, **43**, pp. 484-492. DOI: 10.1016/j.geotexmem.2015.07.014
- [18] Kaliakin V., Khabbazian M., Meehan C., 2012. Modelling the Behaviour of Geosynthetic Encased Columns: Influence of Granular Soil Constitutive Model. *International Journal of Geomechanics*, **12**(4), pp. 357–369. DOI: 10.1061/(ASCE)GM.1943-5622.0000084
- [19] Ambily A., Gandhi S., 2007. Behaviour of Stone Columns Based on Experimental and FEM Analysis. *Journal of Geotechnical and Geo-Environmental Engineering*, **133**(4), pp. 405-415. DOI: 0.1061/(ASCE)1090-0241(2007)133:4(405).